GROUND DATA PROCESSING & PRODUCTION OF THE LEVEL 1 HIGH RESOLUTION MAPS

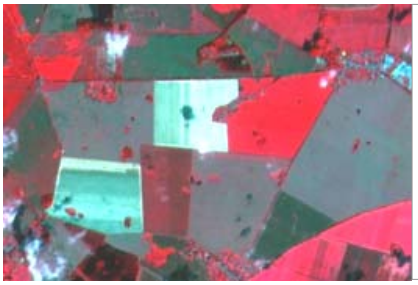

VALERI 2004

Demmin site
(crops)

Philippe Rossello, Frédéric Baret

January 2007

CONTENTS

1. Introduction **2**
2. Available data **2**
2.1. SPOT Image 2
2.2. Hemispherical images 3
2.3. Sampling strategy 5
2.3.1. Principles 5
2.3.2. Evaluation based on NDVI values 6
2.3.3. Using convex hulls 7
2.3.4. Evaluation based on classification 8
3. Determination of the transfer function for the 6 biophysical variables: LAIeff, LAI57eff, LAItrue, LAI57true, fCover, fAPAR **11**
3.1. The transfer function considered 11
3.2. Results 12
4. Conclusion **12**
5. Acknowledgements **12**

1. Introduction

This report describes the production of high resolution, level 1, biophysical variable maps for the Demmin site in 2004. Level 1 map corresponds to the map derived from the determination of a transfer function between reflectance values of the SPOT image acquired during (or around) the ground campaign, and biophysical variable measurements (hemispherical images). For each Elementary Sampling Unit (ESU), the hemispherical images were processed using the CAN-EYE software (version 4.2) developed at INRA-CSE. The derived biophysical variable maps are:

• four Leaf Area Index (LAI) are considered: effective LAI (LAIeff) and true LAI (LAItrue) derived from the measurement of the gap fraction as a function of the view zenith angle; effective LAI57 (LAI57eff) and true LAI57 (LAI57true) derived from the gap fraction at 57.5°, which is independent on the leaf inclination. Effective LAI and effective LAI57 do not take into account clumping effect. LAItrue and LAI57true are derived using the method proposed by Lang and Xiang[1] (1986);

• cover fraction (fCover): it is the percentage of soil covered by vegetation. To improve the spatial sampling, fCover was computed over 0 to 10° zenith angle;

• fAPAR: it is the fraction of Absorbed Photosynthetically Active Radiation (PAR = 400-700nm). fAPAR is defined either instantaneously (for a given solar position) or integrated all over the day. Following a study based on radiative transfer model simulations, it has been shown that the root mean square error between instantaneous fAPAR computed every 30 minutes and the daily fAPAR is the lowest for instantaneous fAPAR at 10h00 AM (solar time, RMSE = 0.021). Therefore, the derivation of fAPAR from CAN-EYE corresponds to the instantaneous black sky fAPAR at 10h00 AM.

The land cover is mainly composed of crops: barley, wheat, corn, grassland, rapeseed, corn, potatoes… The site is approximately 5 km x 3 km with coordinates described in Table 1:

	UTM 33, North, WGS-84 (units = meters)		Geographic Lat/Lon WGS-84 (units = degrees)	
	Easting	Northing	Lat.	Lon.
Upper left corner	379565.0660	5974771.3750	53.90735634	13.16666096
Lower right corner	384805.0660	5971231.3750	53.87674454	13.24771679
Center	382185.0660	5973001.3750	53.89205742	13.20720359

Table 1. Description of the site coordinates: they correspond to SPOT image coordinates.

2. Available data

2.1. SPOT Image

No satellite image (SPOT, Landsat, IRS) without cloud coverage during or around the ground campaign is available. Note that the ground measurements were carried out from 11/06/2004 to 12/06/2004.

However, SPOT image acquired the 23rd July 2004 by HRVIR1 on SPOT4 was ordered to analyse the results. It was geo-located by SPOT image (SPOTView, precision 2B). The projection is UTM 33 North, WGS-84. No atmospheric correction was applied to the image since no atmospheric data were available. However, as the SPOT image is used to compute empirical relationships between reflectance and biophysical variable, we can assume that the effect of the atmosphere is the same over the whole 5 x 3 km site. Therefore, it will be taken into account everywhere in the same way.

Figure 1 shows the relationship between Red and near infrared (NIR) SPOT channels: the soil line is marked and no saturated points are observed.

[1] Lang, A.R.G. and Yueqin, Xiang, Y., 1986. Estimation of leaf area index from transmission of direct sunlight in discontinuous canopies. Agric. For. Meteorol., 37: 229-243.

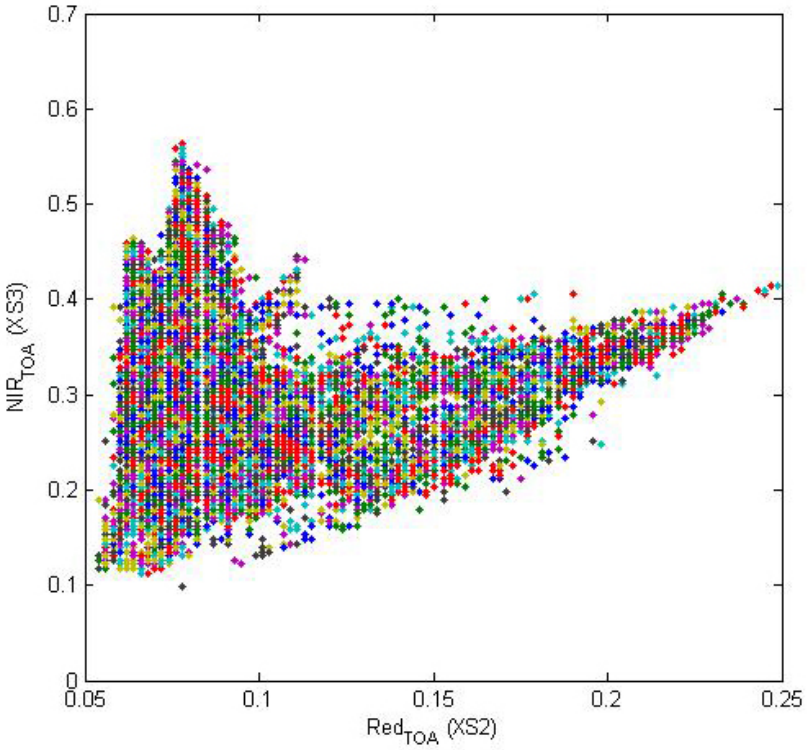

Figure 1. Red/NIR relationship on the SPOT image for Demmin, 2004.

2.2. Hemispherical images

The hemispherical images were processed using the CAN-EYE software (version 4.2) to derive the biophysical variables.

Figure 2 and Figure 3 show the distribution of the several variables over the 36 sampled ESUs. As there was understorey on E31 (forest), hemispherical images were acquired from above the understorey and from below the canopy (trees). The two sets of acquisition were processed separately to derive LAI (effective and true), LAI57 (effective and true), fCover, and fAPAR. The ESU biophysical variable was then computed as:

- LAIeff, LAI57eff, LAItrue, LAI57true: LAI(above) + LAI(below).
- fCover: fCover(above)*fCover(below). This assumes independency between the gaps inside the understorey and those inside the trees which is not true at all the scales but it is the only way to get the total fCover. However, for the local scales considered, this might be true as a first order approximation.
- fAPAR: [1-(1-fAPAR(below))*(1-fAPAR(above))], since 1-fAPAR can be considered equivalent to a gap fraction. Here again, the same independency between the two layers has to be assumed.

Note that LAI (effective and true) derived from directional gap fraction and LAI derived from gap fraction at 57.5° (effective and true) are consistent (Figure 2 and Figure 3). Effective LAI (LAIeff, LAI57eff) varies from 0.02 to 5.67, while true LAI (LAItrue, LAI57true) varies from 0.03 to 8.54. These ranges show quite heterogeneous site in terms of LAI. LAIeff and LAI57eff are lower than LAItrue and LAI57true, due to the clumping observed for several ESUs. The relationship between fAPAR and LAI is in agreement with what is expected (Beer-Lambert law) while the fCover-LAI relationship is more noisy.

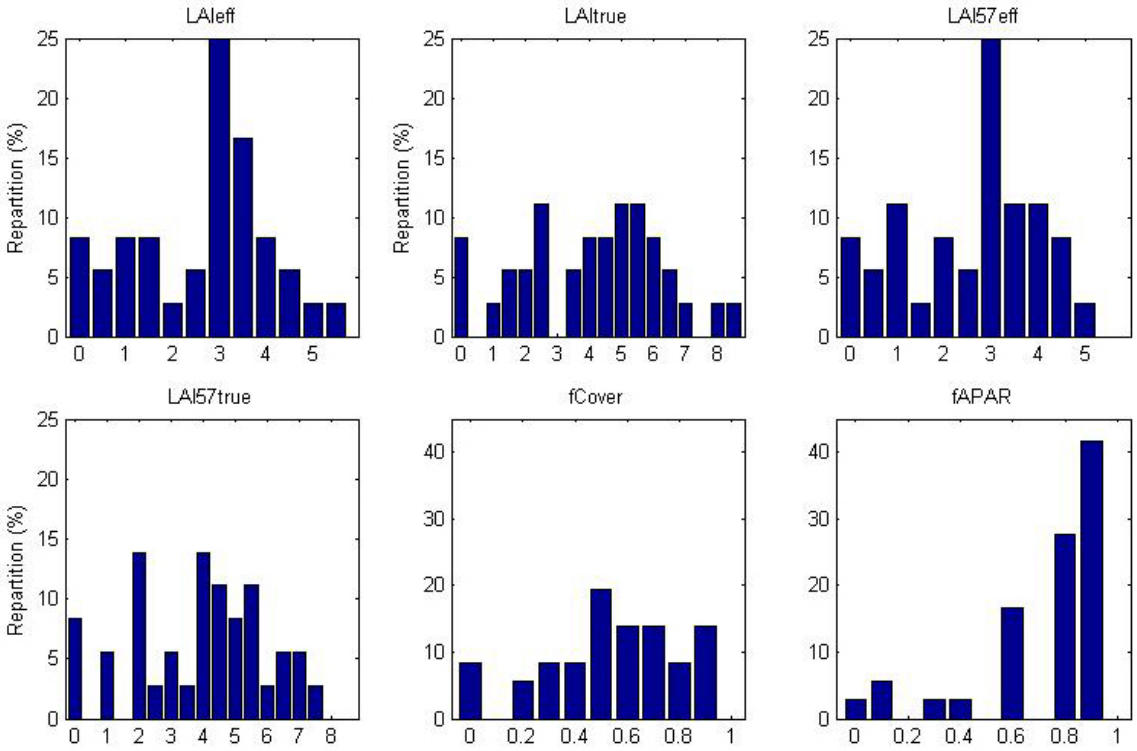

Figure 2. Distribution of the measured biophysical variables over the ESUs.

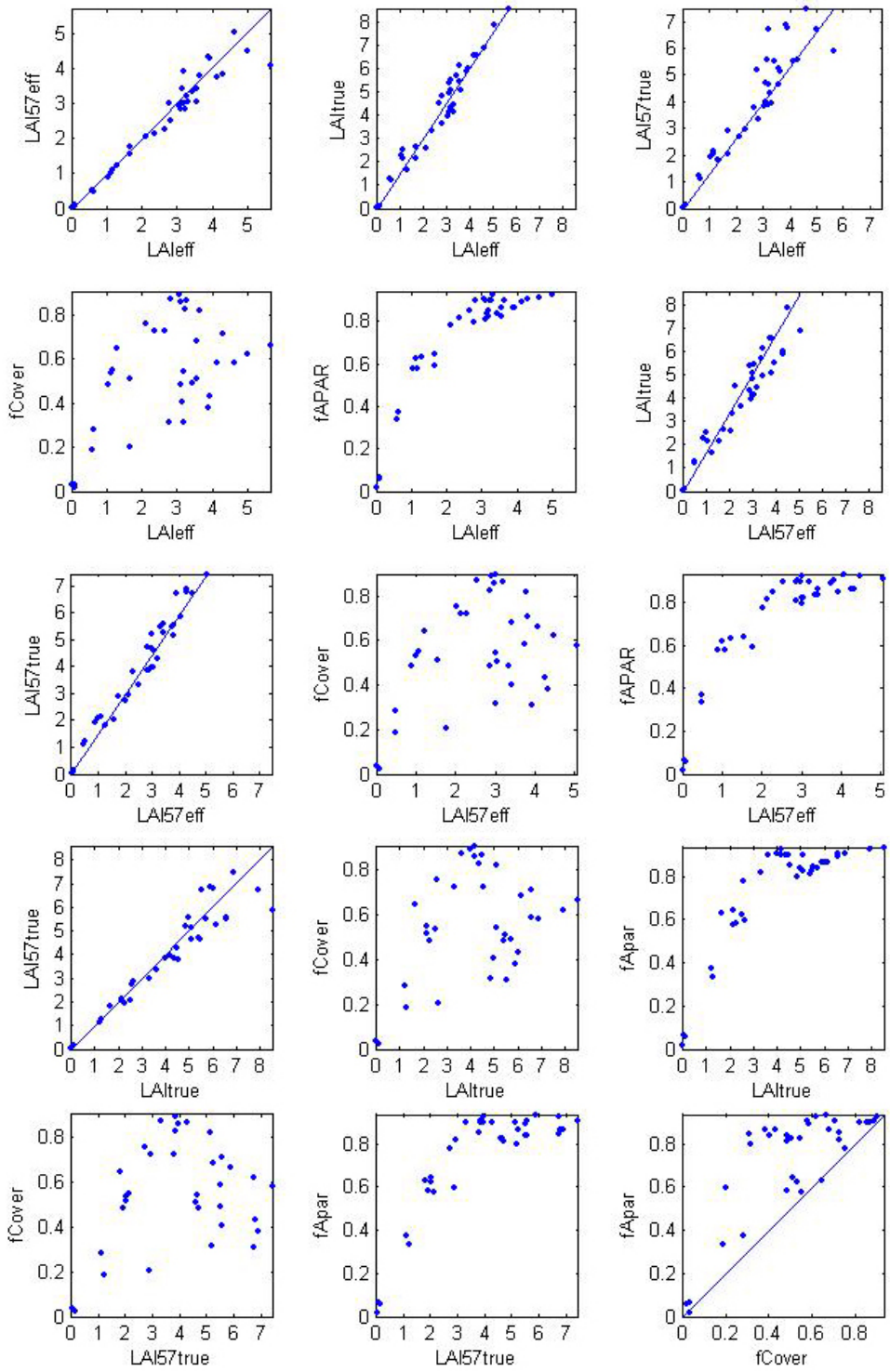

Figure 3. Relationships between the different biophysical variables

2.3. Sampling strategy

2.3.1. Principles

The sampling of each ESU is based on twelve elementary photographs. Figure 4 shows that the 36 ESUs are evenly distributed over the site (5 x 3 km). The processing of the ground data has shown that: considering that SPOT geo-location and GPS measurements are associated to errors, E03, E05, E06, E10, E11, E18, E20 and E32 have been shifted by 1 or 2 SPOT pixels since they were close to a road. Moreover, E11 was located on a small plot with a strong heterogeneity on the borders. It has been also shifted by 2 pixels.

Finally the 36 ESUs have been kept for the computation of the transfer function.

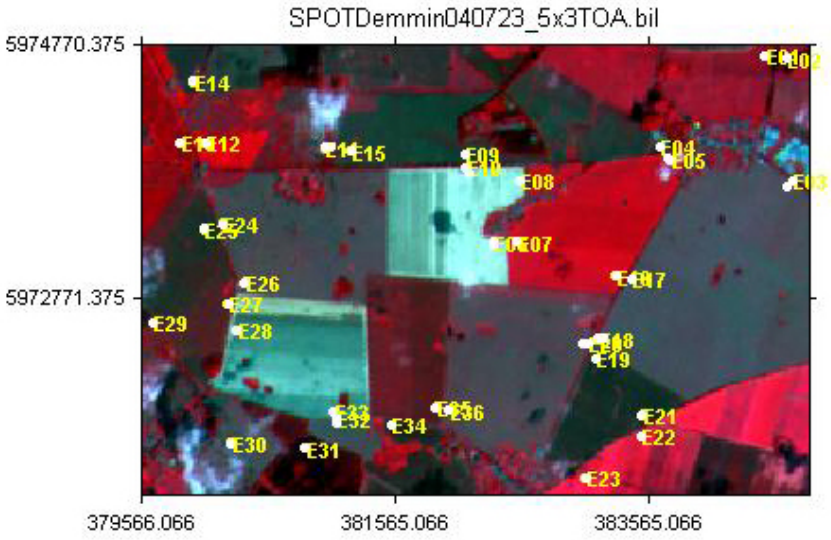

Figure 4. Distribution of the ESUs around the Demmin site.

2.3.2. Evaluation based on NDVI values

The sampling strategy is evaluated using the SPOT image by comparing the NDVI distribution over the site with the NDVI distribution over the ESUs (Figure 5). As the number of pixels is drastically different for the ESU and whole site (WS = 37500 in case of a 5 x 3 km SPOT image at 20 m resolution), it is not statistically consistent to directly compare the two NDVI histograms. Therefore, the proposed technique consists in comparing the NDVI cumulative frequency of the two distributions by a Monte-Carlo procedure which aims at comparing the actual frequency to randomly shifted sampling patterns. It consists in:

1. computing the cumulative frequency of the N pixel NDVI that correspond to the exact ESU locations;
2. then, applying a unique random translation to the sampling design (modulo the size of the image);
3. computing the cumulative frequency of NDVI on the randomly shifted sampling design;
4. repeating steps 2 and 3, 199 times with 199 different random translation vectors.

This provides a total population of $N = 199 + 1$(actual) cumulative frequency on which a statistical test at acceptance probability $1 - \alpha = 95\%$ is applied: for a given NDVI level, if the actual ESU density function is between two limits defined by the $N\alpha/2 = 5$ highest and lowest values of the 200 cumulative frequencies, the hypothesis assuming that WS and ESU NDVI distributions are equivalent is accepted, otherwise it is rejected.

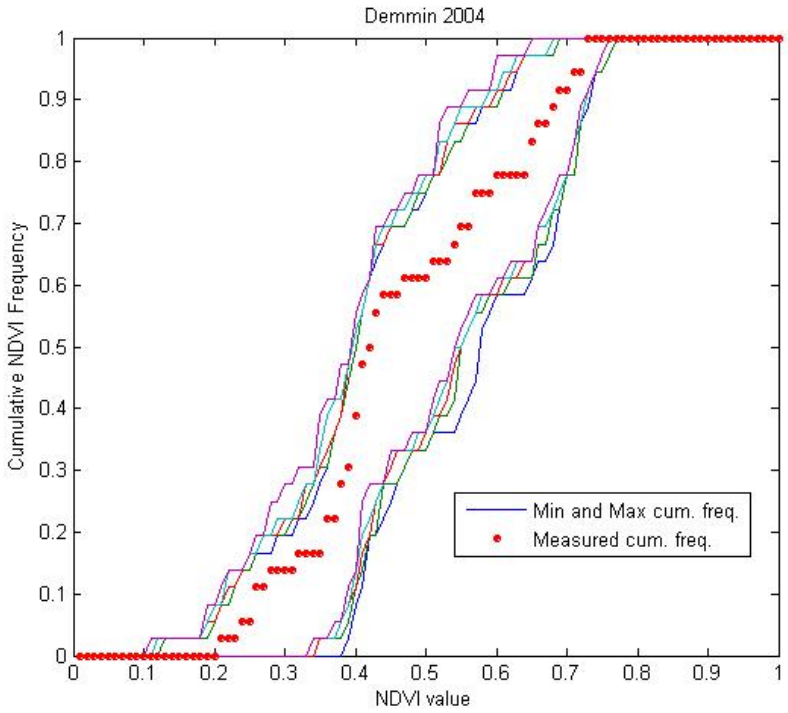

Figure 5. Comparison of the ESU NDVI distribution and the NDVI distribution over the whole image.

Figure 5 shows that the NDVI distribution of the 36 ESUs is very good over the whole site. Note that NDVIs lower than 0.21 have not been sampled although they are present in the image.

2.3.3. Using convex hulls

A test based on the convex hulls was also carried out to characterize the representativeness of ESUs. Whereas the evaluation based on NDVI values uses two bands (red and NIR), this test uses the four bands of the SPOT image. A flag image, is computing over the reflectances (Figure 6). The result on convex-hulls can be interpreted as:

- pixels inside the 'strict convex-hull': a convex-hull is computed using all the SPOT reflectance corresponding to the ESUs belonging to the class. These pixels are well represented by the ground sampling and therefore, when applying a transfer function the degree of confidence in the results will be quite high, since the transfer function will be used as an interpolator;
- pixels inside the 'large convex-hull': a convex-hull is computed using all the reflectance combination (±5% in relative value) corresponding to the ESUs. For these pixels, the degree of confidence in the obtained results will be quite good, since the transfer function is used as an extrapolator (but not far from interpolator);
- pixels outside the two convex-hulls: this means that for these pixels, the transfer function will behave as an extrapolator which makes the results less reliable. However, having a priori information on the site may help to evaluate the extrapolation capacities of the transfer function.

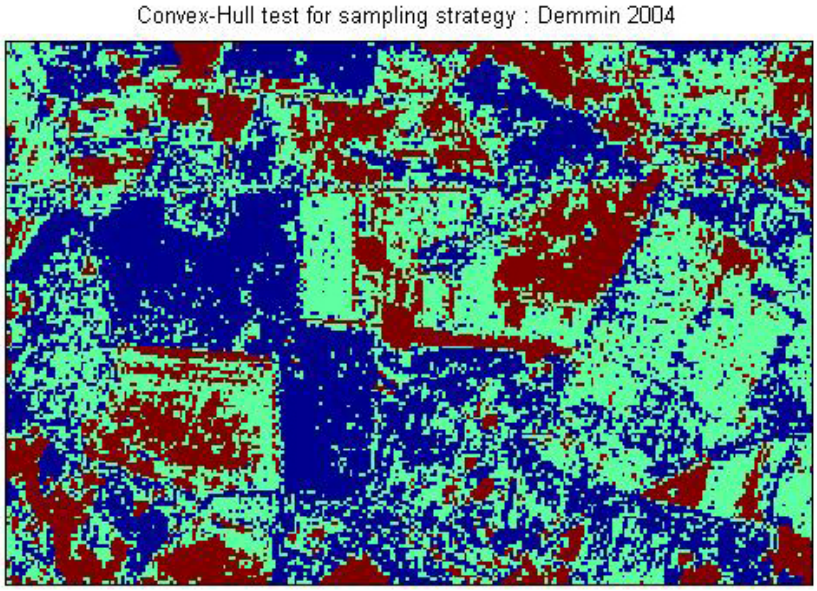

Figure 6. Evaluation of the sampling based on the convex hulls: blue and light blue correspond to the pixels belonging to the 'strict' and 'large' convex hulls and red to the pixels for which the transfer function is extrapolating.

This map shows that the representativeness of the ESUs is good, even if pixels are outside the two convex-hulls. They mainly correspond to grassland, sugar beet, forest, urban surfaces, bare soil…

2.3.4. Evaluation based on classification

A non supervised classification based on the k_means method (Matlab statistics toolbox) was applied to the reflectance of the SPOT image to distinguish if different behaviours on the image for the biophysical variable-reflectance relationship exist.

A number of 4 classes was chosen (Figure 7). The distribution of the classes on the image and on the ESUs is rather similar.

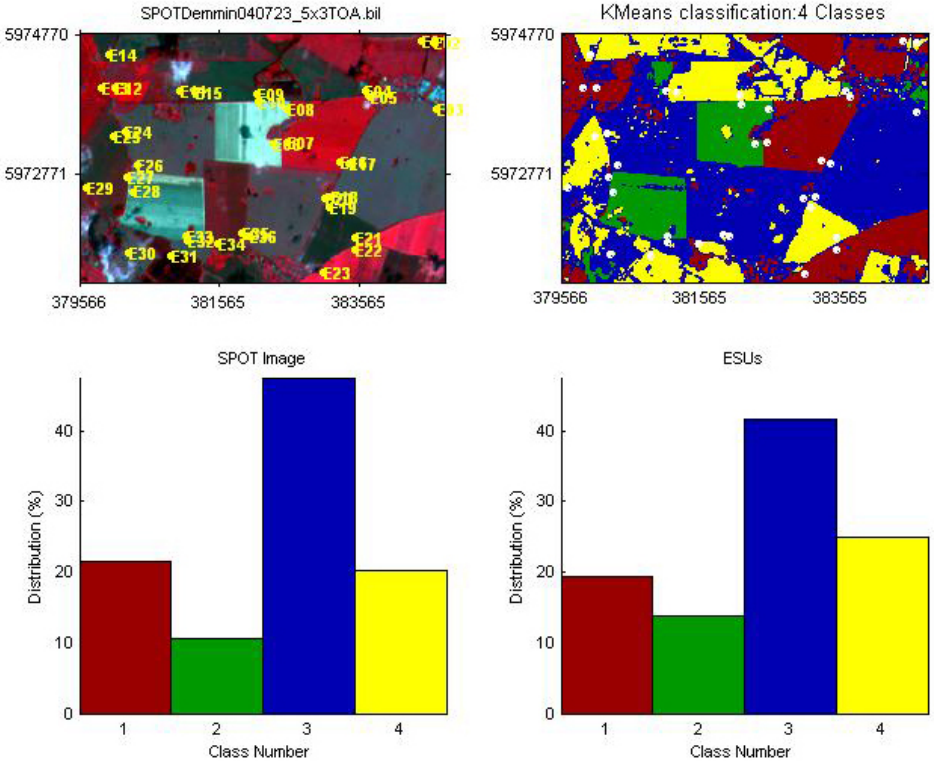

Figure 7. Classification of the SPOT image. Comparison of the class distribution between the SPOT image and sampled ESUs.

Figure 8 shows the different relationships observed between the biophysical variables and the corresponding NDVI on the ESUs, as a function of the SPOT classes determined from non supervised classification:

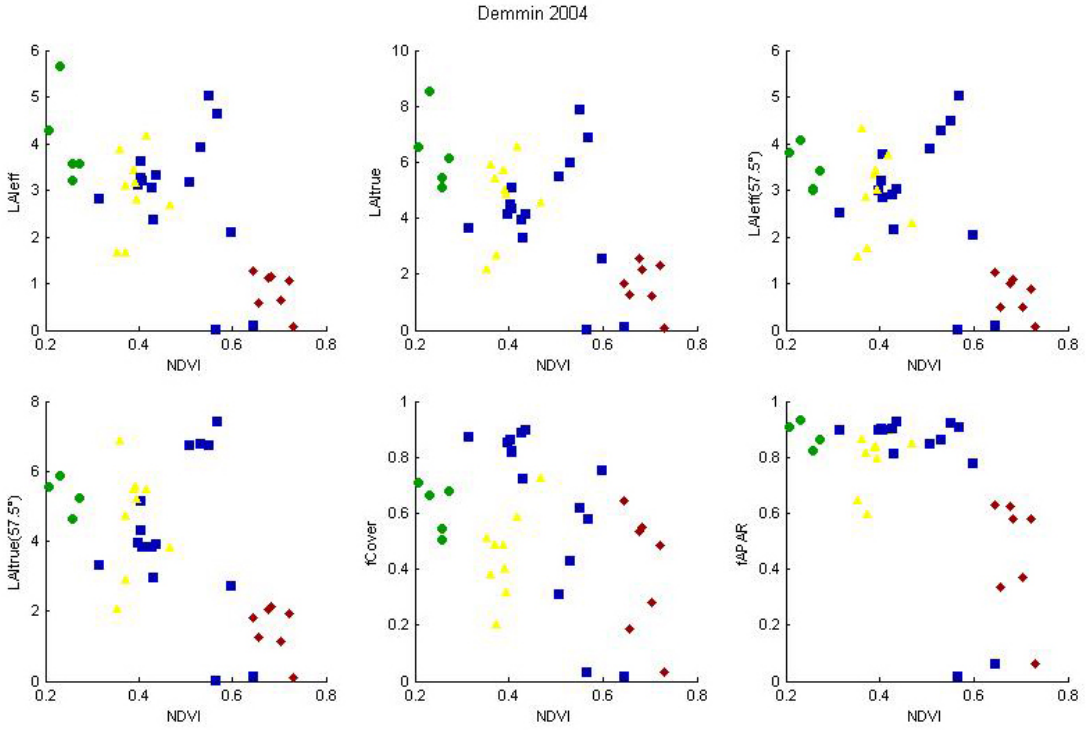

Figure 8. NDVI-Biophysical Variable relationships as a function of SPOT classes

There is no relation between NDVI and biophysical variables. This is due to the date of data acquisition: the ground measurements were carried out the 11th and 12th June whereas the SPOT image was acquired the 23rd July.

As the relationship between LAI and NDVI is not significant, the biophysical variable maps cannot be derived from the determination of a transfer function between reflectance values of the satellite image acquired and biophysical variable measurements. However, a land cover map (Figure 10) was performed from SPOT image acquired the 23rd July 2004[2], ground observations during the campaign and a topographic map[3] (Figure 9) kindly provided by Rainer Ressl.

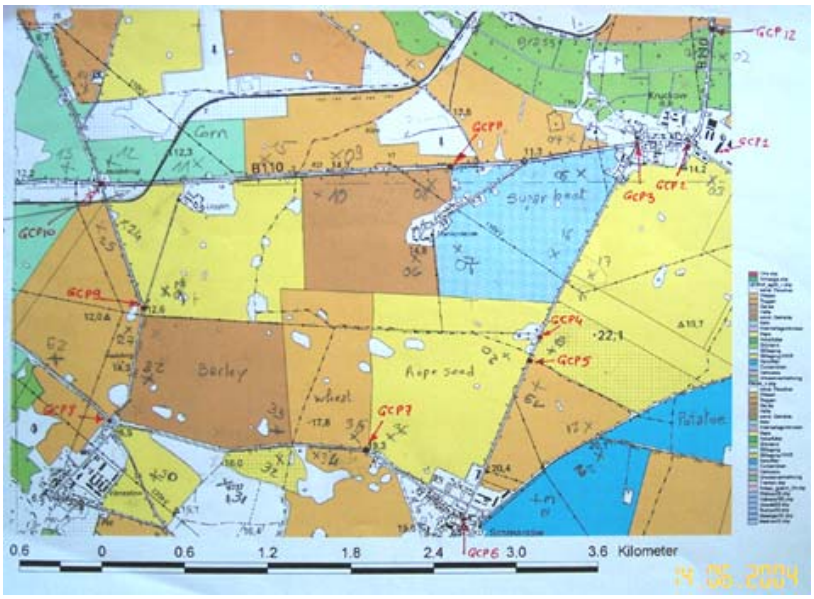

Figure 9. Topographic map describing the land cover of Demmin site

[2] Information provided from unsupervised classification, segmentation…
[3] Mecklenburg-Vorpommern, scale 1:10000

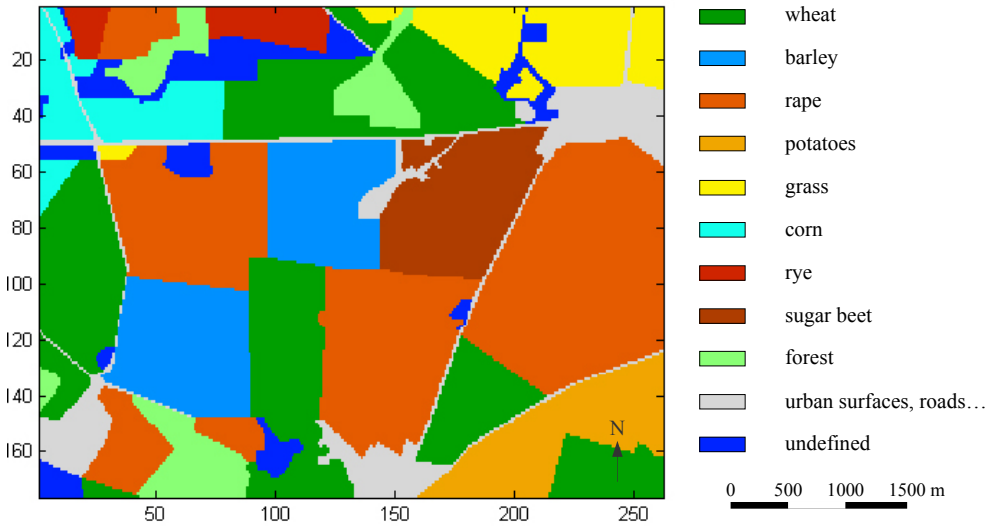

Figure 10. The land cover map produced from SPOT image (23rd july 2004), ground observations during the campaign and a topographic map of Demmin site

Eleven classes (Figure 11) characterize the land cover map produced from SPOT image, ground observations during the campaign and the topographic map: “wheat” (10 ESUs), “barley” (5), “rape” (9), “potatoes” (2), “grass” (2), “corn” (3), “rye” (1), “sugar beet” (3), “forest” (1), “urban surfaces…” (0), “undefined” (0). Note that 5% of the land cover map are undefined since a few small areas were not sampled.

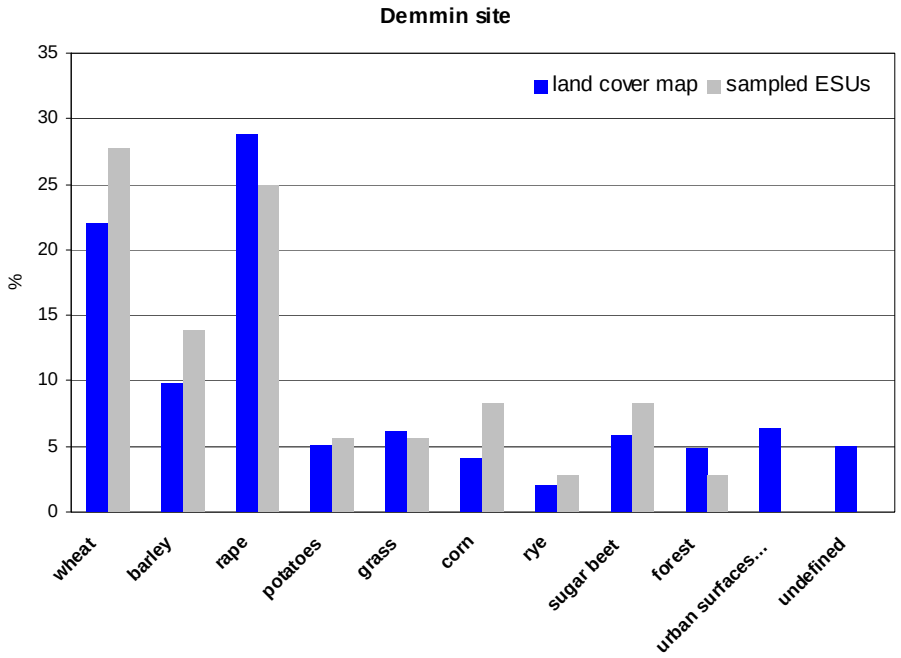

Figure 11. Comparison of the class distribution between the land cover map and sampled ESUs

The distribution of the classes on the image and on the ESUs is quite similar, even if classes “wheat”, “barley”, “corn”, “sugar beet” are over-sampled and classes “rape”, ”forest” are under-represented. Note that there are not sampled ESUs which characterize “urban surfaces” and “undefined” (NaN value attributed to this class).

As SPOT image was used for support to build the land cover map, the projection and the resolution are the same. The land cover map at high resolution (20 m) is thus used to provide biophysical variable maps (LAI, fCover, fAPAR), even if, for some marginal classes, the accuracy is not optimal. A simple transfer function is generated in order to produce biophysical variable maps at high resolution.

3. Determination of the transfer function for the 6 biophysical variables: LAIeff, LAI57eff, LAItrue, LAI57true, fCover, fAPAR

3.1. The transfer function considered

As the satellite image is not suitable because of the time delay with ground measurements, the following method is applied: for each class, the transfer function consists in attributing the average value of the biophysical variable measured on the class to each pixel of the land cover map belonging to the class.

For urban class, LAIeff and fAPAR values are estimated from NDVI based methods. Note that NDVI values are estimated from the high spatial resolution SPOT image acquired the 23rd July 2004. This implicitly assumes NDVI is considered constant on urban surfaces between the 12th June and the 23rd July. As no atmospheric correction was applied to the SPOT image, maximum NDVI value ($NDVI_{max}$) corresponds to the average of highest NDVI values (2% of the image) and minimum NDVI value ($NDVI_{min}$) corresponds to the average of lowest NDVI values (2% of the image):

- ***effective LAI***

$$LAIeff = -1/K_{LAI}.\ln[(NDVI-NDVI_{max})/(NDVI_{min}-NDVI_{max})]$$ Weiss[4], M. *and al.,* 2002

where

$NDVI_{max}$ is the maximum NDVI value = 0,73

$NDVI_{min}$ is the minimum NDVI value = 0,19

K_{LAI} is the extinction coefficient = 0,67.

- ***fAPAR***

$$fAPAR = fAPAR_{max}*1-[(NDVI-NDVI_{max})/(NDVI_{min}-NDVI_{max})]$$ Baret, F., and Guyot G.[5], 1991

where

$fAPAR_{max}$ = 0,94

$NDVI_{max}$ is the maximum NDVI value = 0,73

$NDVI_{min}$ is the minimum NDVI value = 0,19

[4] Weiss, M., F. Baret, M. Leroy, O. Hautecoeur, C. Bacour, L. Prévot, and N. Bruguier. 2002. Validation of neural net techniques to estimate canopy biophysical variables from remote sensing data. Agronomie, 22:547-554.

[5] Baret, F., and G. Guyot. 1991. Potentials and limits of vegetation indices for LAI and APAR assessment. Remote Sensing of the Environment, 35:161-173.

3.2. Results

The results of the transfer function are displayed on table 2:

		wheat	barley	rape	potatoes	grass	corn	rye	sugar beet	forest	urban surfaces, roads…	undefined	
	nb ESUs	10	5	9	2	2	3	1	3	1	0	0	
LAIeff	min	1.66	3.2	1.66	0.59	1.28	0.02	-	1.05	-	0	-	
	max	5.02	5.67	3.64	0.64	2.11	0.1	-	1.14	-	5.571	-	
	std	0.905	0.881	0.564	0.025	0.415	0.033	-	0.04	-	0.724	-	
	mean	**3.474**	**4.056**	**2.942**	**0.615**	**1.695**	**0.063**	**4.15**	**1.107**	**2.66**	**1.399**	**NaN**	
LAItrue	min	2.67	5.09	2.16	1.2	1.66	0.03	-	2.15	-	-	-	
	max	7.91	8.54	5.1	1.28	2.57	0.12	-	2.54	-	-	-	
	std	1.298	1.207	0.784	0.04	0.455	0.037	-	0.161	-	-		
	mean	**5.578**	**6.35**	**3.931**	**1.24**	**2.115**	**0.077**	**6.56**	**2.33**	**4.54**	**NaN**	**NaN**	
LAI57eff	min	1.76	3.01	1.57	0.48	1.24	0.02	-	0.89	-	-	-	
	max	5.04	4.08	3.78	0.5	2.03	0.09	-	1.08	-	-	-	
	std	0.912	0.423	0.6	0.01	0.395	0.029	-	0.078	-	-		
	mean	**3.638**	**3.472**	**2.778**	**0.49**	**1.635**	**0.057**	**3.74**	**0.993**	**2.27**	**NaN**	**NaN**	
LAI57true	min	2.88	4.62	2.03	1.13	1.83	0.03	-	1.94	-	-	-	
	max	7.44	5.87	5.14	1.24	2.71	0.14	-	2.12	-	-	-	
	std	1.296	0.493	0.822	0.055	0.44	0.045	-	0.075	-	-		
	mean	**5.837**	**5.182**	**3.709**	**1.185**	**2.27**	**0.087**	**5.49**	**2.04**	**3.79**	**NaN**	**NaN**	
fCover	min	0.203	0.506	0.512	0.187	0.645	0.02	-	0.483	-	-	-	
	max	0.62	0.709	0.9	0.282	0.7562	0.033	-	0.55	-	-	-	
	std	0.121	0.081	0.115	0.047	0.0556	0.006	-	0.029	-	-		
	mean	**0.422**	**0.621**	**0.806**	**0.235**	**0.701**	**0.028**	**0.584**	**0.522**	**0.723**	**NaN**	**NaN**	
fAPAR	min	0.593	0.822	0.642	0.336	0.631	0.015	-	0.577	-	0	-	
	max	0.923	0.935	0.927	0.372	0.778	0.064	-	0.622	-	0.948	-	
	std	0.087	0.045	0.084	0.018	0.074	0.022	-	0.021	-	0.177		
	mean	**0.828**	**0.87**	**0.865**	**0.354**	**0.704**	**0.046**	**0.892**	**0.593**	**0.849**	**0.531**	**NaN**	
	surface (%)	22.1	9.8	28.7	5.1	6.1	4.1	2.1	5.8	4.9	6.4	5	100

Table 2. Transfer function applied to the whole site for the different biophysical variables

Note that the "undefined" class corresponds to plots or areas which are not strictly identified. It covers 5% of the site.

4. Conclusion

No satellite high spatial resolution image without clouds during or around the ground campaign was available. The closest clear sky image was a SPOT image acquired the 23rd July 2004, but the relationship between LAI and NDVI was not significant. This is due to the time delay with ground measurements carried out the 11th and 12th June. Therefore, the biophysical variable maps were not produced from transfer functions using reflectance values of the high spatial resolution SPOT image and ground measurements. More simple transfer functions were derived from a land cover map which is derived itself from the SPOT image, labeling of the fields by ground survey and a topographic map. The transfer function developed over 36 ESUs consists in attributing the average value of the biophysical variable measured on the class to each pixel of the land cover map belonging to the class. Note that the Demmin site, as an agriculture site, is heterogeneous in terms of LAI.

The biophysical variable maps are available in UTM, 33 North, projection coordinates (Datum: WGS-84) at 20 m resolution.

5. Acknowledgements

We want to thank: **Rainer Ressl**, **Erik Borg** (German Aerospace Center, Germany) and **Frédéric Baret** (INRA-CSE, Avignon) for the organisation and participation to the campaign.